

# Septin 14 Is Involved in Cortical Neuronal Migration via Interaction with Septin 4

Tomoyasu Shinoda, Hidenori Ito, Kaori Sudo, Ikuko Iwamoto, Rika Morishita, and Koh-ichi Nagata

Department of Molecular Neurobiology, Aichi Human Service Center, Institute for Developmental Research, Kasugai, Aichi 480-0392, Japan

Submitted October 15, 2009; Revised February 12, 2010; Accepted February 17, 2010  
Monitoring Editor: Josephine C. Adams

Septins are a family of conserved guanosine triphosphate/guanosine diphosphate-binding proteins implicated in a variety of cellular functions such as cell cycle control and cytokinesis. Although several members of septin family, including Septin 14 (Sept14), are abundantly expressed in nervous tissues, little is known about their physiological functions, especially in neuronal development. Here, we report that Sept14 is strongly expressed in the cortical plate of developing cerebral cortex. Knockdown experiments by using the method of in utero electroporation showed that reduction of Sept14 caused inhibition of cortical neuronal migration. Whereas cDNA encoding RNA interference-resistant Sept14 rescued the migration defect, the C-terminal deletion mutant of Sept14 did not. Biochemical analyses revealed that C-terminal coiled-coil region of Sept14 interacts with Septin 4 (Sept4). Knockdown experiments showed that Sept4 is also involved in cortical neuronal migration in vivo. In addition, knockdown of Sept14 or Sept4 inhibited leading process formation in migrating cortical neurons. These results suggest that Sept14 is involved in neuronal migration in cerebral cortex via interaction with Sept4.

## INTRODUCTION

Septins are a family of heteropolymeric filament-forming guanine nucleotide-binding proteins originally discovered in a screen for genes involved in cell division of budding yeast (Hartwell, 1971). Subsequent studies identified septins in most eukaryotic organisms, with the exception of plants (Kinoshita *et al.*, 1997; Oegema *et al.*, 1998; Nguyen *et al.*, 2000). Septins have been implicated in several cellular functions such as cell cycle control, cytokinesis, mitotic spindle formation, and plasma membrane compartmentalization (Longtine *et al.*, 1996; Field and Kellogg, 1999; Trimble, 1999; Barral and Kinoshita, 2008). The accumulating biochemical and cell biological observations in lower eukaryotic septins suggest that they may function through the assembly of diffusion barriers (Takizawa *et al.*, 2000; Dobbelaere and Barral, 2004) or as scaffolds (Lew, 2003; Spiliotis and Nelson, 2006).

In mammals, 14 septin genes have been identified. Recent studies reported abundant expression of septins in neuronal tissues (Kinoshita *et al.*, 2000; Ito *et al.*, 2009). Several septins are found to accumulate in postsynaptic density fractions of brain, by mass spectrometry analyses (Peng *et al.*, 2004; Collins *et al.*, 2006). These septins are suggested to be involved in dendritic maturation, including spine morphogenesis and synaptic connectivity in cultured hippocampal neurons (Tada *et al.*, 2007; Xie *et al.*, 2007; Li *et al.*, 2009). The

physiological functions of septins in neurons, however, still remain largely unknown.

The coordinated migration of neurons is essential for functional and architectural formation of mammalian brain. During corticogenesis, postmitotic neurons generated in the ventricular zone (VZ) move through the intermediate zone (IZ) and arrive at the superficial layers of the cortical plate (CP) (Rakic, 1990; Gleeson and Walsh, 2000; Hatten, 2002). Disturbance of this migration process can cause misplacement of neurons and result in disorganized cortical lamination, a defect observed in neurological disorders such as mental retardation and epilepsy (Clark, 2002). Analyses based on the human and mouse genetics have suggested the implication of several genes, such as *Reelin*, *LIS1*, *DCX*, and *CDK5*, in neuronal migration (Gupta *et al.*, 2002; Olson and Walsh, 2002). Such simple genetic approaches, however, seem not to be sufficient for the elucidation of molecular mechanisms underlying cortical development, because mutations in genes potentially involved in corticogenesis may cause severe abnormality in earlier developmental events, thereby result in lethality before cortical development. In utero electroporation method (Inoue and Krumlauf, 2001; Saito and Nakatsuji, 2001; Tabata and Nakajima, 2001) is a promising solution for the problem. This method allows us to perform acute expression or knockdown of genes of interest in neuronal precursor cells in embryonic cerebral cortex, followed by observation of the cell shape, migration and proliferation of transfected neurons in subsequent developmental stages.

In the present study, by using this approach, we examined the function of Septin 14 (Sept14), a member of septin family molecules abundantly expressed in developing cerebral cortex, in neuronal development. We show that Sept14 is involved in neuronal migration through the interaction with Sept4. Furthermore, we identify a role of Sept14 and Sept4 in the formation of neuronal process.

This article was published online ahead of print in *MBoC in Press* (<http://www.molbiolcell.org/cgi/doi/10.1091/mbc.E09-10-0869>) on February 24, 2010.

Address correspondence to: Koh-ichi Nagata (knagata@inst-hsc.jp).

Abbreviations used: CP, cortical plate; IZ, intermediate zone; SVZ, subventricular zone; VZ, ventricular zone.

## MATERIALS AND METHODS

### Plasmids

cDNA encoding mouse Sept14 and Sept3 was obtained by polymerase chain reaction (PCR) from mouse brain cDNA library. The cDNA encoding Sept14 full (amino acids [aa] 1-467), Sept14 $\Delta$ CC (aa 1-366), Sept14CC (aa 367-467), Sept4, or Sept3 was inserted into pCAG-FLAG-MCS2 or pCAG-myc-MCS2, modified vectors of pCAG-MCS2 (Kawauchi *et al.*, 2005). Enhanced green fluorescent protein (EGFP)-expression vector pGAG-EGFP was kindly provided by Drs. Hoshino (National Institute of Neuroscience, Tokyo, Japan) and Kawauchi (Keio University, Tokyo, Japan). cDNA encoding mouse Sept4 was kindly provided by Dr. Kinoshita (Nagoya University, Nagoya, Japan).

### Primary Antibodies

Antibodies against green fluorescent protein (GFP) (rabbit polyclonal; MBL, Aichi, Japan; rat monoclonal, Nakarai, Kyoto, Japan), NeuN (mouse monoclonal; Millipore Bioscience Research Reagents, Temecula, CA), Nestin (mouse monoclonal; BD Biosciences, Franklin Lakes, NJ), tau-1 (mouse monoclonal; Millipore Bioscience Research Reagents),  $\beta$  III-tubulin (mouse monoclonal; Millipore Bioscience Research Reagents), microtubule-associated protein 2 (mouse monoclonal; Sigma-Aldrich, St. Louis, MO),  $\beta$ -tubulin (mouse monoclonal; Sigma-Aldrich), 5-bromo-2-deoxyuridine (BrdU, mouse monoclonal; Sigma-Aldrich), myc (mouse monoclonal; Santa Cruz Biotechnology, Santa Cruz, CA), and FLAG (mouse monoclonal and rabbit polyclonal; Sigma-Aldrich) were purchased. Rabbit polyclonal antibodies against Sept6, Sept7, and Sept11 were prepared as described previously (Hanai *et al.*, 2004; Nagata *et al.*, 2004; Ito *et al.*, 2009). We generated a rabbit polyclonal antibody against mouse Sept14 by using maltose-binding protein-fused C-terminal region (aa 321-467) expressed in *Escherichia coli* as an antigen. Rabbit polyclonal antibodies against Sept3 and Sept4 were kindly provided by Drs. M. Takehashi (Osaka Ohtani University, Osaka, Japan) and M. Kinoshita (Nagoya University), respectively.

### Small Interfering RNAs (siRNAs)

25mer siRNA duplexes (Stealth RNAi; Invitrogen, Carlsbad, CA) were designed to target two distinct regions in the Sept14 coding sequence (Sept14-siRNA#1, 5'-CCTACAGAGGTTCAAGAACAACATA-3'; Sept14-siRNA#2, 5'-GAGGAGGTCAAAGTTGGAAAGAGAA-3'), two distinct regions in the Sept4 coding sequence (Sept4-siRNA#1, 5'-CGGATCATGCAAACCGTG-GAGATTA-3'; Sept4-siRNA#2, 5'-ACGGGGTCAACATTGTGCCTATCTT-3'), and one region in the Sept3 coding sequence (Sept3-siRNA, 5'-CCCTG-GAGGAGAAGTCGGAATCAA-3'). Stealth RNA interference (RNAi)

Negative Control Medium GC Duplex #2 (Invitrogen) was used as a negative control. To generate an RNAi-resistant mutant of Sept14 (Sept14<sup>R</sup>) and Sept14 $\Delta$ CC (Sept14 $\Delta$ CC<sup>R</sup>), we introduced four silent mutations, as underlined, in the target sequence of Sept14-siRNA#1 (5'-CCTTCAAAGGTTTAA-GAACAAATATA-3'). To generate an RNAi-resistant mutant of Sept4 (Sept4<sup>R</sup>), three silent mutations are introduced in the target sequence of Sept4-siRNA#1 (5'-CGGATGATGCAGACAGTGGAGATTA-3').

### In Utero Electroporation

All animal experiments were performed according to the guidance of the Institute for Developmental Research. Pregnant ICR mice were purchased from SLC Japan (Sizuoka, Japan). In utero electroporation was performed as described previously (Tabata and Nakajima, 2001), with some modifications. In brief, 2  $\mu$ l of nucleotide solution containing expression plasmid (2  $\mu$ g) and siRNA (20 pmol) was introduced into lateral ventricles of embryos, followed by electroporation using CUY21 electroporator (NEPA Gene, Chiba, Japan) with 50 ms of 30-V electronic pulse for 6 times with 950-ms intervals. All electroporations in this report were performed on embryonic day 14.5 (E14.5).

### Immunohistochemistry

The developing brains fixed with 4% paraformaldehyde (PFA) were sectioned coronally with Vibratome (Leica, Wetzlar, Germany) at 100  $\mu$ m for E13.5 and E15.5, 70  $\mu$ m for E17.5 and postnatal day 2 (P2), and 50  $\mu$ m for P10. The slices were treated with phosphate-buffered saline (PBS) containing 2% goat serum and 0.5% Triton X-100 for 1 h, and subsequently incubated with diluted primary antibodies in PBS at 4°C overnight. After several washes with PBS, slices were treated with Alexa488- or Alexa568-conjugated secondary antibodies diluted in PBS for 1 h at 4°C. In some experiment, nuclei were visualized by 4',6-diamino-2-phenylindole (DAPI) (Nakarai). Fluorescent images were obtained by laser scanning confocal microscopy (FV1000; Olympus, Tokyo, Japan).

### BrdU Incorporation Experiment

Embryos were electroporated in utero at E14.5. 30 h after electroporation. Pregnant mice were given two intraperitoneal injections of BrdU at 50 mg/kg body weight, with a 30-min interval. 1 h after the first injection, embryonic brains were fixed. Vibratome sections were immunostained with anti-GFP and Alexa488-conjugated secondary antibody. After being briefly fixed with 4% PFA, sections were treated with 2 N HCl for 30 min at 37°C followed by the immunostaining with anti-BrdU and Alexa568-conjugated secondary antibody.

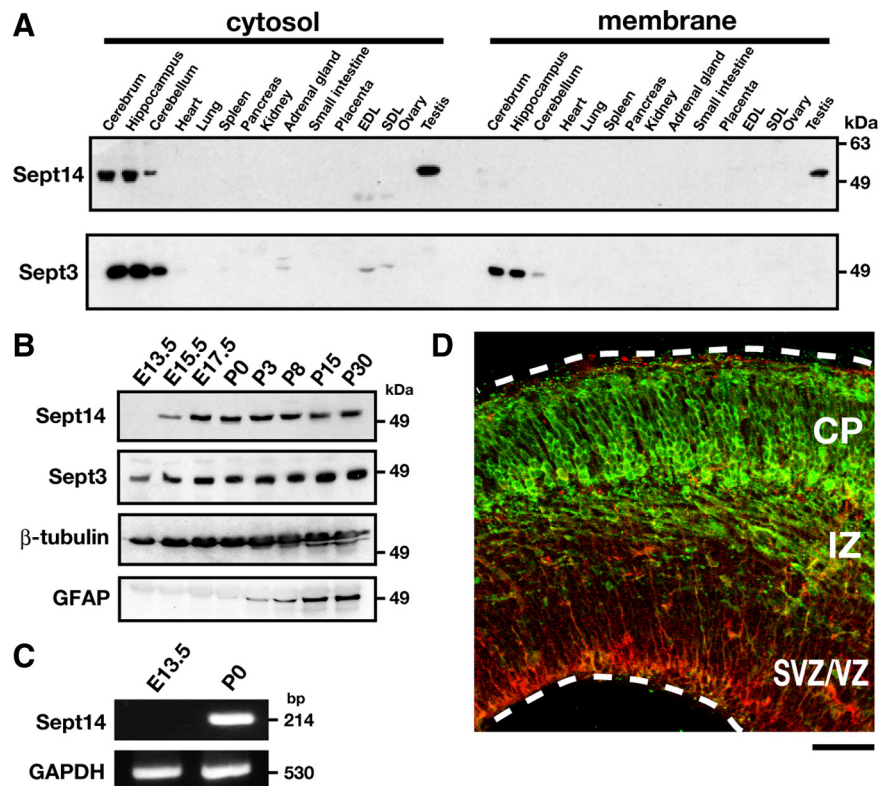


**Figure 1.** Expression profile of Sept14. (A) Cytosolic (20  $\mu$ g protein/lane) and membrane (30  $\mu$ g protein/lane) fractions from adult mice organs were separated by SDS-PAGE and subjected to immunoblotting with anti-Sept14 or anti-Sept3. EDL, extensor digitorum longus muscle; SOL, soleus muscle. (B) Whole lysates of cerebral cortices at various developmental stages (50  $\mu$ g protein/lane) were subjected to SDS-PAGE and immunoblotting with antibodies against indicated proteins. (C) RT-PCR was performed to amplify Sept14- or GAPDH-specific product from total RNA isolated from cerebral cortex of E13.5 or P0 mice. (D) Coronal section of E15.5 mouse cerebral cortex was immunostained with anti-Sept14 (green) and anti-Nestin (red). Bar, 100  $\mu$ m.

### Quantitative Estimation of Neuronal Migration and Leading Process Formation

The distribution of EGFP-positive or EGFP/FLAG double-positive cells in brain slices was quantified as follows. The coronal sections of cerebral cortices containing the labeled cells were classified into four regions, layer II-IV, V-VI, IZ, and the subventricular zone (SVZ)/VZ, as described previously (Kawauchi *et al.*, 2003). The number of labeled cells in each region of at least four slices per brain was calculated. To measure the length of leading process of migrating neurons, images of EGFP-positive neurons in the lower CP were acquired by laser scanning confocal microscopy. Postmigratory neurons in the superficial CP were excluded from the assay. At least seven independent brains were electroporated and analyzed for each experiment.

### Primary Culture and Immunocytochemistry

Primary culture of mouse cortical and hippocampal neurons was performed as described previously (Kawauchi *et al.*, 2006; Shinoda *et al.*, 2007). In some experiments, cerebral cortices electroporated at E14.5 were dissociated at E17.5 and cultured. Transfection into primary cultured neurons was performed by Nucleofector (Amaxa Biosystems, Cologne, Germany), according to the manufacturer's protocol. Neurons were fixed with 3.7% formaldehyde in PBS for 10 min and treated with PBS containing 0.05% Triton X-100 for 10 min. Neurons were incubated with primary antibodies overnight at 4°C, washed, and incubated for 1 h with secondary antibodies. Fluorescent images were obtained by laser scanning confocal microscopy.

### Preparation of Various Mouse Tissues

Various tissues and brain regions were dissected from adult ICR mice. Cytosol and membrane extracts of tissues were prepared as described previously

(Ito *et al.*, 2002). To analyze the developmental expression profiles of septins, whole extracts of cerebral cortices of embryonic and postnatal mice were prepared with 3 volumes of buffer L (20 mM Tris-HCl, 150 mM NaCl, 1% NP-40, 0.5% deoxycholate, 0.1% SDS, 10 µg/ml leupeptin, and 10 µM phenylmethylsulfonyl fluoride, pH 7.4) and subjected to SDS-polyacrylamide gel electrophoresis (PAGE) and immunoblotting. Concentrations of protein were calculated with bicinchoninic acid protein assay kit (Pierce Chemical, Rockford, IL).

### Reverse Transcription (RT)-PCR

Total RNA was isolated from cerebral cortex of E13.5 or P0 mice by ISOGEN RNA extraction kit (Nippon Gene, Tokyo, Japan). PCR primers were designed as follows: 5'-AGGCCGGTGCTGAGTATGTC-3' and 5'-TGCCTGCTTCAC-CACCTTCT-3' for mouse *GAPDH* and 5'-TCGCTTCAAAGAACGACCT-3' and 5'-AAACTCCCAAGGTAATGG-3' for mouse *Sept14*. RT-PCR was performed with SuperScript one-step RT-PCR kit (Invitrogen) according to the manufacturer's protocol.

### Yeast Two-Hybrid Analysis

pYTH9-mouse *Sept14* was used as a bait in the two-hybrid screen with human brain cDNA library fused to pACT2 (BD Biosciences), following the Matchmaker two-hybrid system protocol (Clontech, Mountain View, CA). Subsequent two-hybrid interaction analyses were carried out as described previously (Nagata *et al.*, 1998).

### Immunoprecipitation Analyses

COS7 cells were transfected with Lipofectamine (Invitrogen), according to the manufacturer's protocol. Transfected COS7 cells were lysed with buffer L.

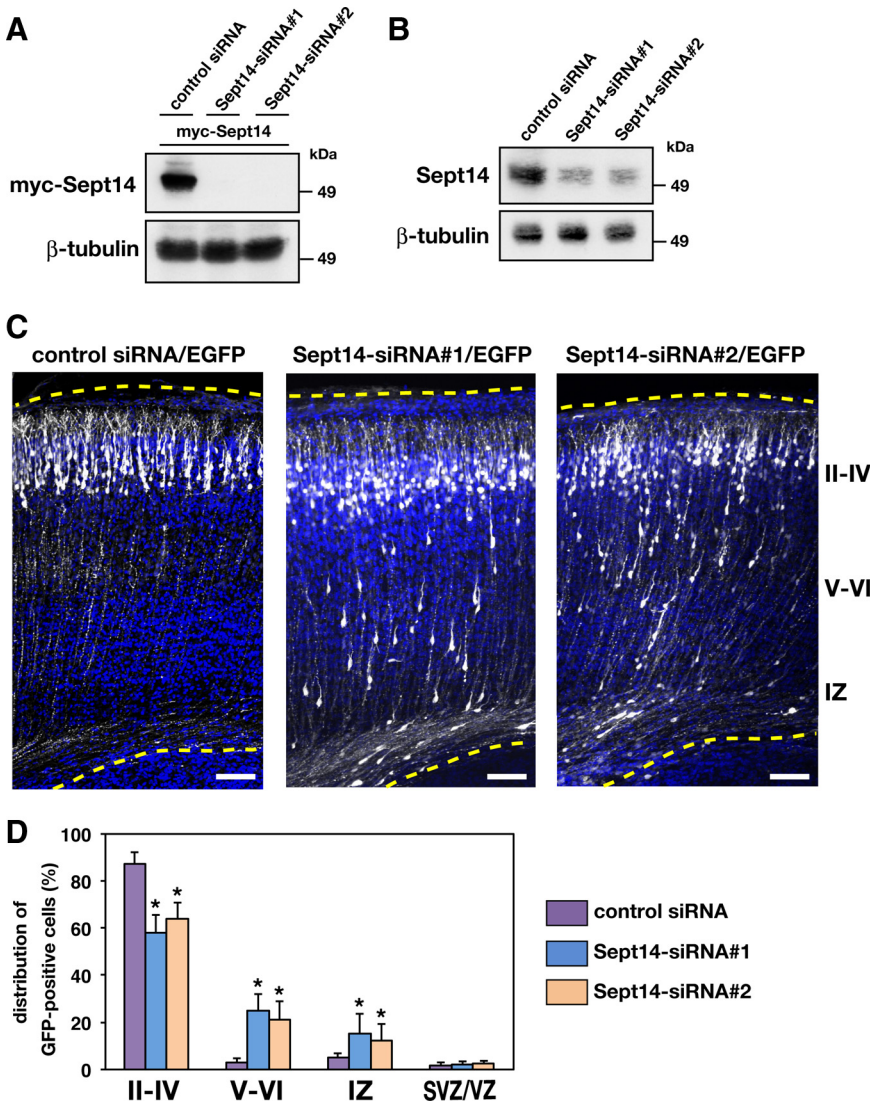


**Figure 2.** Roles of Sept14 in neuronal migration. (A) pCAG-myc-Sept14 was cotransfected into COS7 cells with control siRNA, Sept14-siRNA#1 or Sept14-siRNA#2. After 72 h, cells were lysed and subjected to immunoblotting with anti-myc or anti-β-tubulin. (B) Cortical neurons were transfected with control siRNA, Sept14-siRNA#1, or Sept14-siRNA#2. After 72 h, cells were lysed and subjected to immunoblotting with anti-Sept14 or anti-β-tubulin. (C) pCAG-EGFP was coelectroporated with control siRNA, Sept14-siRNA#1, or Sept14-siRNA#2 into cerebral cortices at E14.5 and fixed at P2. Coronal sections were immunostained with anti-GFP (white). Nuclei were stained with DAPI (blue). Dotted lines represent pial and ventricular surfaces. Bars, 100 µm. II-IV, layers II-IV of CP; V-VI, layers V and VI of CP. (D) Quantification of the distribution of EGFP-positive cells in distinct parts of the cerebral cortex (layer II-IV, layer V-VI, IZ, and SVZ/VZ) for each condition shown in C. Error bars indicate SD. \*p < 0.01, percentage of cells in each region relative to the corresponding values with control condition.

Cell lysates were incubated with anti-FLAG or anti-myc for 45 min at 4°C, followed by additional incubation for 45 min with protein A-Sepharose (GE Healthcare, Little Chalfont, Buckinghamshire, United Kingdom). The beads were washed three times with buffer L, and the bound proteins were subjected to SDS-PAGE and immunoblotting. For the precipitation of endogenous Sept14, control immunoglobulin (Ig)G, or anti-Sept14 was cross-linked to protein A-Sepharose beads by BS3 (Thermo Fisher Scientific, Waltham, MA) according to the manufacturer's protocol. Whole extract of cerebral cortices from P2 mice was prepared with 3 volumes of buffer L and then incubated with the cross-linked beads for 45 min at 4°C. Bound proteins were eluted with SDS sample buffer and analyzed by immunoblotting.

## RESULTS

### Distribution of Sept14 in Mouse Tissues

To elucidate biological functions of Sept14, we generated a polyclonal antibody against Sept14 and examined the Sept14-expression profile in adult mouse tissues. Immunoblot analyses revealed strong cytosolic expression of Sept14 in brain, including cerebrum, hippocampus and cerebellum, and testis (Figure 1A). We next examined the expression profile of Sept14 during cerebral cortex development. Although Sept14 was not detected at E13.5 (Figure 1B), it was visualized around E15.5 and then dramatically increased and reached the maximal level around E17.5 (Figure 1B). RT-PCR analyses of *Sept14* transcription supported its developmental expression in cerebral cortex (Figure 1C). We also examined the expression of Sept14 in embryonic cerebral cortex by immunohistochemistry. Little immunoreactivity was observed in E13.5 cortex (data not shown), which was consistent with the result of immunoblot analyses (Figure 1B). In E15.5 cortex, Sept14 was observed predominantly in upper IZ and CP, but very weakly in SVZ and VZ (Figure 1D). Considering that CP and IZ at this developmental stage contain migrating neurons, these results suggest a possibility that Sept14 is involved in the radial neuronal migration during corticogenesis.

### Roles of Sept14 in Neuronal Migration

To investigate the function of Sept14 in neuronal migration, we sought to decrease the expression of Sept14 by RNAi with *in utero* electroporation. We designed two siRNAs, Sept14-siRNA#1 and Sept14-siRNA#2, against distinct regions of mouse *Sept14* coding sequence. Both siRNAs effectively knocked down the expression of myc-Sept14 in COS7 cells (Figure 2A). We next transfected these siRNAs into dissociated cortical neurons and cultured for 3 d. Immunoblot analysis revealed that both Sept14-siRNA#1 and Sept14-siRNA#2 significantly decreased the amount of endogenous Sept14 (Figure 2B). Knockdown of Sept14 was also confirmed by immunocytochemistry in cortical neurons (Supplemental Figure 1). To examine the possible function of Sept14 in neuronal migration, siRNAs and pCAG-EGFP were coelectroporated into VZ cells at E14.5. The animals were killed at P2 to observe the localization of transfected cells and their progeny. Most control siRNA-transfected neurons normally migrated to the superficial layers of the cortical plate (Figure 2, C and D). In contrast, a considerable portion of cells transfected with Sept14-siRNA#1 or Sept14-siRNA#2 remained in layer V to IV of CP and in IZ (Figure 2, C and D). It should be noted that many Sept14-siRNAs-transfected neurons reached the superficial layer of CP (Figure 2B), possibly attributable to the limited RNAi effect of these siRNAs. The defective positioning of Sept14-siRNAs-transfected neurons in the ventricular side of CP was still observed in the mice analyzed at P10 (Supplemental Figure 2; data not shown).

We next examined whether the observed mislocalization of neurons results from a possible effect of Sept14-siRNAs on

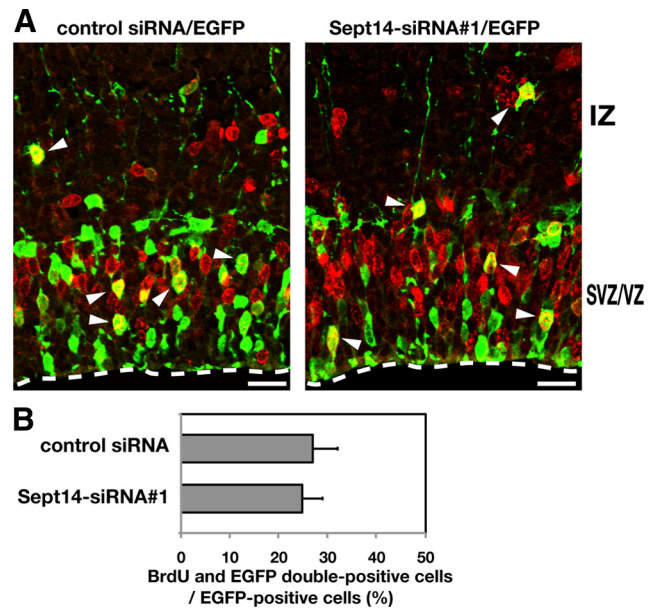


**Figure 3.** Effect of Sept14-silencing on cell division in VZ. (A) E14.5 cortices were coelectroporated with pCAG-EGFP together with control siRNA or Sept14-siRNA#1. BrdU incorporation was examined as described in *Materials and Methods*. Coronal sections of brains were immunostained by anti-GFP (green) and anti-BrdU (red). Arrowheads indicate BrdU/EGFP double-positive cells. Dotted lines represent ventricular surface. Bars, 50  $\mu$ m. (B) Quantification of BrdU/EGFP double-positive cells among EGFP-positive cells. Error bars indicate SD.

neuronal proliferation. After pCAG-EGFP was electroporated into E14.5 embryos with control siRNA or Sept14-siRNA#1, pregnant mice were subjected to intraperitoneal injection of BrdU at E15.5. Embryos were then killed 1 h after the injection to observe the BrdU incorporation. Consequently, the incorporation rate was not statistically different between control and Sept14-siRNA#1-introduced cells (Figure 3, A and B). Moreover, positioning of the BrdU/EGFP-double positive cells within VZ and SVZ was not affected by the transfection of Sept14-siRNA#1 (Figure 3A). Together with the result that the expression of Sept14 in cerebral cortex at E15.5 was limited in CP and upper IZ (Figure 1D), neuronal positioning defect by Sept14-siRNAs is most likely to attribute to abnormality in cell migration rather than proliferation.

### Identification of Sept4 as a Sept14-binding Protein

To investigate the molecular basis of the function of Sept14 on neuronal migration, we attempted to identify binding partners for Sept14. We performed a yeast two-hybrid screen with Sept14 as a bait and a cDNA library from human brain. Subsequent DNA sequence analyses revealed that Sept4, another septin molecule specifically expressed in brain and testis (Kinoshita *et al.*, 1998; Ihara *et al.*, 2005) is a candidate binding partner for Sept14, as suggested recently (Peterson *et al.*, 2007).

We examined the expression profile of Sept4 in developing cerebral cortex. A constant expression of Sept4 was observed from E13.5 to P30 by immunoblotting (Figure 4A). Immunohistochemistry revealed that the expression of Sept4 was predominantly observed in IZ and CP at E15.5 (Figure 4B). To confirm the interaction between Sept14 and Sept4, immunoprecipitation analyses were performed using the

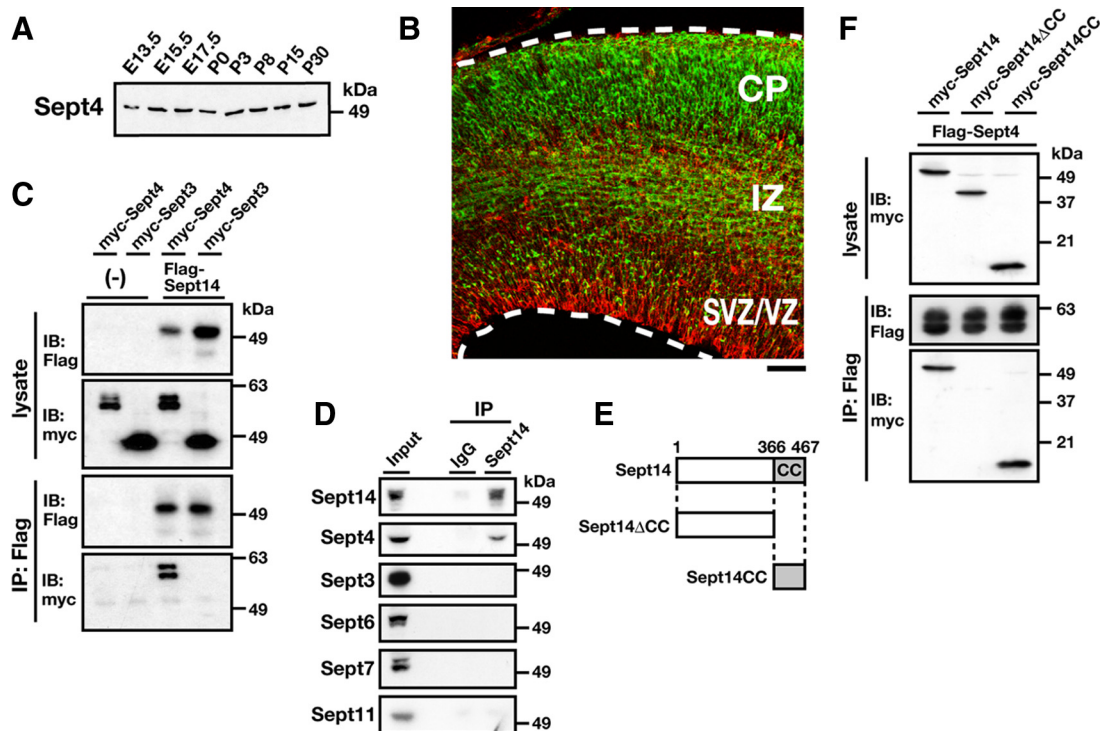


**Figure 4.** Interaction of Sept14 with Sept4. (A) Whole lysates of mouse cerebral cortices at various developmental stages were subjected to SDS-PAGE and immunoblotting with anti-Sept4. (B) Coronal section of E15.5 mouse cerebral cortex was immunostained with anti-Sept4 (green) and anti-Nestin (red). Bar, 100  $\mu$ m. (C) COS7 cells were cotransfected with FLAG-Sept14, myc-Sept4, and myc-Sept3 in the indicated combinations and cultured for 48 h. Cells were then lysed and subjected to immunoprecipitation with anti-FLAG. Cell lysates (lysate) and precipitated materials (IP: FLAG) were subjected to immunoblotting with anti-myc or anti-FLAG. (D) Lysate of mouse cerebral cortices were immunoprecipitated with anti-Sept14. Samples were then subjected to immunoblotting with anti-Sept14, -Sept4, -Sept3, -Sept6, -Sept7, or -Sept11. (E) Two deletion mutants of Sept14 used in this study are shown. CC, coiled-coil domain. (F) COS7 cells were cotransfected with FLAG-Sept4, myc-Sept14, myc-Sept14 $\Delta$ CC, and myc-Sept14CC in the indicated combinations and cultured for 48 h. Cells were lysed and immunoprecipitated with anti-FLAG. Immunoblotting was done as described in C.

COS7 cell expression system. Consequently, myc-Sept4 was coprecipitated with FLAG-Sept14 (Figure 4C). In contrast, myc-Sept3, a brain-specific septin (Figure 1A), did not associate with FLAG-Sept14 under the conditions used (Figure 4C). We also examined the interaction of endogenous Sept14 with Sept4 by immunoprecipitation. When Sept14 was precipitated from mouse brain lysate, Sept4 was detected in the precipitate (Figure 4D). Sept3, Sept6, Sept7, and Sept11, in contrast, did not coprecipitate with Sept14 under these conditions (Figure 4D). These results suggest that Sept14 forms a complex with Sept4 in physiological conditions. We next tried to determine the binding region of Sept14 to Sept4. Because the C-terminal coiled-coil region in septin is important for the interaction with other septin molecules (Scheffield *et al.*, 2003; Nagata *et al.*, 2004; Low and Macara, 2006), we generated two Sept14 mutants, Sept14 $\Delta$ CC and Sept14CC (Figure 4E). Myc-Sept14 $\Delta$ CC was not coprecipitated with FLAG-Sept4 under conditions in which wild-type Sept14 and Sept14CC associates with Sept4 (Figure 4F). These results suggest that the C-terminal coiled-coil region of Sept14 is responsible for interaction with Sept4.

#### Involvement of Sept4 as Well as Sept14 in Neuronal Migration

Because Sept4 is expressed in developing cortex and interacts with Sept14, we speculate that Sept4, as well as Sept14, is involved in neuronal migration in the cerebral cortex. To examine this possibility, we first designed two siRNA du-

plexes, Sept4-siRNA#1 and Sept4-siRNA#2, to target distinct regions in the *Sept4* coding sequence. Both siRNAs effectively knocked down the expression of myc-Sept4 in COS7 cells (Figure 5A), and endogenous Sept4 in cortical neurons (Figure 5B and Supplemental Figure 3). To examine whether Sept4 is involved in neuronal migration, siRNAs and pCAG-EGFP were coelectroporated into VZ cells at E14.5. When analyzed at P2, many Sept4-siRNA#1- or Sept4-siRNA#2-transfected neurons were abnormally located in layer V to layer IV of CP and IZ (Figure 5, C and D). This phenotype was very similar to that observed in Sept14-knockdown experiments (Figure 2, C and D). These results strongly suggest that Sept4, as well as Sept14, is required for the proper positioning of cortical neurons during corticogenesis. It is notable that silencing of Sept3 did not affect the positioning of cortical neurons (Supplemental Figure 4). It seems that not all septins expressed in the developing brain are implicated in proper neuronal positioning.

We next examined whether the knockdown of Sept14 has a synergistic effect on Sept4 knockdown. To this end, both Sept4-siRNA#1 and Sept14-siRNA#1 were coelectroporated at E14.5 and observation was performed at P2. The distribution of cells transfected with both siRNAs, however, was not significantly different from that of each single knock-down (Figures 2D and 5D). Thus, it is not likely that Sept14 and Sept4 synergistically function in neuronal migration, at least based on a loss-of-function assay.

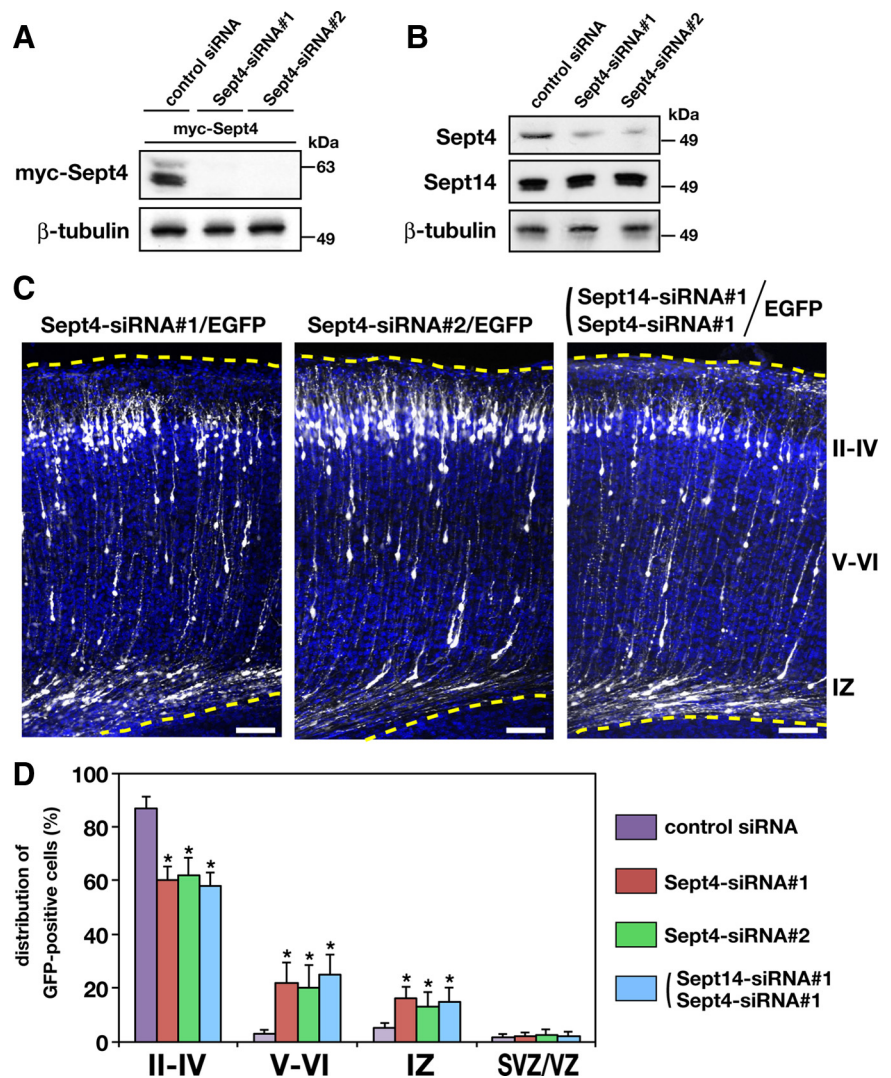


**Figure 5.** Functional role of Sept4 in neuronal migration. *A*, COS7 cells were cotransfected with pCAG-myc-Sept4 together with control siRNA, Sept4-siRNA#1, or Sept4-siRNA#2. After 72 h, cells were lysed and subjected to immunoblotting with anti-myc or anti- $\beta$ -tubulin. *B*) Cortical neurons were transfected with control siRNA, Sept4-siRNA#1, or Sept4-siRNA#2. After 72 h, cells were lysed and subjected to immunoblotting with anti-Sept4, anti-Sept14, or anti- $\beta$ -tubulin. *C*) pCAG-EGFP was coelectroporated with Sept4-siRNA#1, Sept4-siRNA#2, or Sept14-siRNA#1 into cerebral cortices at E14.5, followed by fixation at P2. Coronal sections were prepared and immunostained with anti-GFP (white). Nuclei were stained with DAPI (blue). Dotted lines represent pial and ventricular surfaces. Bars, 100  $\mu$ m. *D*) Quantification of the distribution of EGFP-positive cells in distinct parts of the cerebral cortex (layer II-IV, layer V-VI, IZ, and SVZ/VZ) for each experimental condition shown on the right. Error bars indicate SD. \* $p < 0.01$ , percentage of cells in each region relative to the corresponding values with control condition.

As a next set of experiments, we performed rescue experiments on Sept14 knockdown. We generated vectors expressing siRNA-resistant form of Sept14 (Sept14<sup>R</sup>) and its truncated mutant (Sept14 $\Delta$ CC<sup>R</sup>) that harbor four silent mutations within the sequence targeted by Sept14-siRNA#1. Immunoblot analyses confirmed the resistance of both FLAG-Sept14<sup>R</sup> and FLAG-Sept14 $\Delta$ CC<sup>R</sup> to Sept14-siRNA#1 in COS7 cells (Figure 6A). We next coelectroporated pCAG-EGFP and Sept14-siRNA#1 together with pCAG-FLAG-Sept14<sup>R</sup> or -FLAG-Sept14 $\Delta$ CC<sup>R</sup> into E14.5 cerebral cortices. Majority of EGFP/FLAG-Sept14<sup>R</sup> double-positive cells were located in the superficial layer of CP at P2 (Figure 6, B and C), suggesting that the positional defects by Sept14 knockdown were rescued by expression of exogenous Sept14. The expression of FLAG-Sept14 $\Delta$ CC<sup>R</sup>, in contrast, was not able to rescue the phenotype induced by knockdown of Sept14 (Figure 6, B and C), suggesting an essential role of the coiled-coil domain of Sept14. To further confirm the importance of the coiled-coil domain, we coelectroporated pCAG-EGFP with control pCAG vector or pCAG-FLAG-Sept14CC, which potentially exerts a dominant-negative effect. Consequently, EGFP/FLAG double-positive cells were more frequently observed in layer V to IV of CP and in IZ compared with control experiment (Figure 7, A and B). Considering that the coiled-coil region of Sept14 is responsible for inter-

action with Sept4 (Figure 4F), these results suggest that Sept14 is involved in neuronal migration via interaction with Sept4.

#### Involvement of Sept4 and Sept14 in Leading Process Formation

Newborn cortical neurons generated from VZ primarily exhibit multipolar shapes in the lower part of IZ. The neurons then transform into a bipolar shape with a leading process in the upper part of IZ and migrate into CP toward pial surface (Tabata and Nakajima, 2003; Noctor *et al.*, 2004). We next examined whether Sept14 and Sept4 are involved in the morphogenesis of migrating neurons. pCAG-EGFP were coelectroporated with control siRNA, Sept14-siRNA#1, or Sept4-siRNA#1 at E14.5, and the morphology of migrating neurons in the lower CP were observed at E17.5. The distribution of EGFP-positive cells in cerebral cortex was much less different at this stage among all experimental conditions (data not shown). Sept14-siRNA#1- or Sept4-siRNA#1-transfected bipolar cells in the lower CP exhibited shorter leading processes, compared with control siRNA-transfected cells (Figure 8, A-D). In contrast, the morphology of multipolar cells in IZ was not affected by the transfection of Sept14-siRNA#1 or Sept4-siRNA#1 (data not shown). These

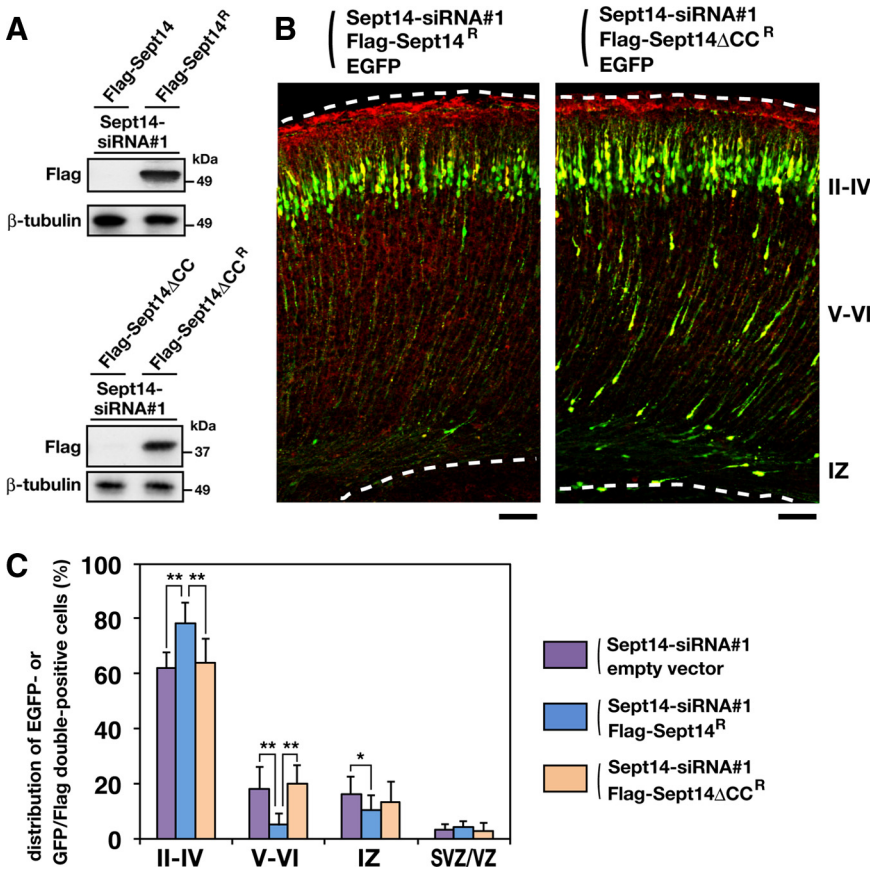


**Figure 6.** Rescue of Sept14-siRNA-induced migration defect. (A) COS7 cells were cotransfected with Sept14-siRNA#1 together with FLAG-Sept14, FLAG-Sept14<sup>R</sup>, FLAG-Sept14ΔCC, or FLAG-Sept14ΔCC<sup>R</sup>. After 72 h, cells were lysed and subjected to immunoblotting with anti-FLAG or anti-β-tubulin. (B) siRNA, pCAG-EGFP, and FLAG-tagged Sept14 mutants were coelectroporated into cerebral cortices in the indicated combinations at E14.5, followed by fixation at P2. Coronal sections were prepared and immunostained with anti-GFP (green) and anti-FLAG (red). Dotted lines represent pial and ventricular surfaces. Note that immunoreactivity of FLAG in the marginal zone and pial surface is artificial background. Bars, 100 μm. (C) Quantification of the distribution of EGFP-positive cells (cotransfection of siRNA, EGFP and empty vectors) or EGFP/FLAG double-positive cells (cotransfection of siRNA, EGFP, and FLAG-Sept14<sup>R</sup> or FLAG-Sept14ΔCC<sup>R</sup> vectors) in distinct parts of the cerebral cortex (layer II–IV, layer V–VI, IZ, and SVZ/VZ) for each experimental condition. Error bars indicate SD. \*\*p < 0.01 and \*p < 0.05, percentage of cells in each region.

results suggest that Sept14 and Sept4 are involved in leading process formation in migrating neurons.

We further examined the roles of Sept14 and Sept4 in process formation by using primary cultured hippocampal neurons, which exhibit highly polarized morphology (Craig and Banker, 1994). Both Sept14 and Sept4 distributed throughout soma, axon, and dendrite (Supplemental Figure 5). Transfection of Sept14-siRNA#1 or Sept4-siRNA#1 resulted in the reduction of primary axon length and total length of dendrites (Figure 9, A–C). The number of primary axons, in contrast, were not affected by the knockdown of Sept14 or Sept4 (Figure 9D). The observed phenotypes by knockdown were rescued by the coexpression of siRNA-resistant form of Sept14 (Sept14<sup>R</sup>) or Sept4 (Sept4<sup>R</sup>) (Supplemental Figure 6). We also examined whether Sept14 depletion affect the distribution of Sept4. Transfection of Sept14-siRNA#1 or Sept14-siRNA#2 did not alter the cytoplasmic distribution of endogenous Sept4 (Supplemental Figure 7). These results suggest that Sept14 and Sept4 are involved in process formation in neuronal cells, rather than cell autonomous polarity formation.

## DISCUSSION

To date, the expression profiles of mammalian septins in various tissues have been widely reported. Some septins are predominantly distributed in neuronal tissues, whereas others are ubiquitously expressed (Kinoshita *et al.*, 2000; Xue *et al.*, 2004; Tada *et al.*, 2007; Ito *et al.*, 2009). Human SEPT14 has been reported to be specifically expressed in testis, based on Northern blotting and RT-PCR analyses (Peterson *et al.*, 2007). In this study, we detected expression of mouse Sept14

in developing central nervous tissues and testis by immunoblotting (Figure 1, A and B), RT-PCR (Figure 1C), immunohistochemistry (Figure 1D), and immunocytochemistry (Supplemental Figure 1). Because the results obtained are consistent with each other and two siRNAs against distinct regions of mouse *Sept14* effectively silenced endogenous Sept14 in neurons (Figures 2B and Supplemental Figure 1), we conclude that Sept14 is expressed in developing brain, at least in mice.

It has so far been reported that expression of several septins is developmentally regulated in cerebral cortex; the protein levels of Sept2, Sept5, Sept6, Sept7, and Sept8 gradually increase at late embryonic stage through early postnatal days (Tada *et al.*, 2007; Ito *et al.*, 2009). In this study, we showed that expression of mouse Sept14 in cerebral cortex is also regulated in the embryonic stage. Although the expression was not detected before E13.5 (Figure 1B; data not shown), a dramatic increase was observed in CP around E15.5 and thereafter (Figure 1, B–D; data not shown). It is thus possible that Sept14 is not only involved in neuronal migration but also in neuronal maturation, including spine morphogenesis and synaptic contact, like other septins (Tada *et al.*, 2007; Xie *et al.*, 2007; Li *et al.*, 2009).

Directed migration of neurons during corticogenesis is an essential event for brain development. In humans, disruption of the ordered neuronal migration leads to cortical malformations, including lissencephaly and periventricular heterotopia. In this study, we report that Sept14 and Sept4 are involved in neuronal migration and morphogenesis during corticogenesis. Although previous studies suggested the requirement of septins in migration of nonneuronal cells (Finger *et al.*, 2003; Hu *et al.*, 2008), the underlying molecular

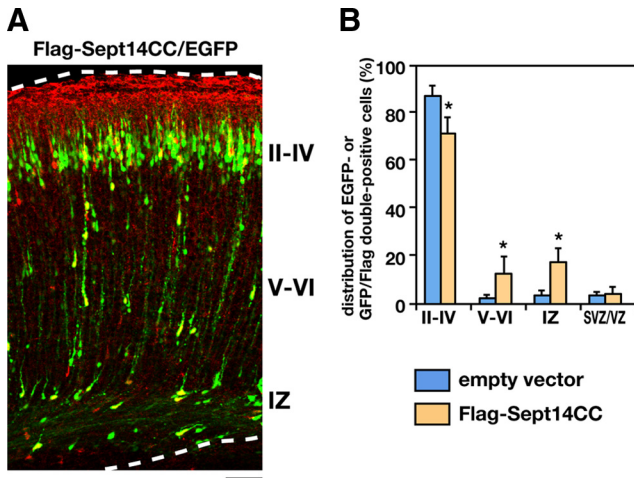


**Figure 7.** Impaired neuronal distribution by the expression of the coiled-coil domain of Sept14. (A) pCAG-EGFP and -FLAG-Sept14CC were coelectroporated into cerebral cortices at E14.5, followed by fixation at P2. Coronal sections were prepared and immunostained with anti-GFP (green) and anti-FLAG (red). Dotted lines represent pial and ventricular surfaces. Bar, 100  $\mu$ m. (B) Quantification of the distribution of EGFP-positive cells (cotransfection of EGFP and empty vectors) or EGFP/FLAG double-positive cells (cotransfection of EGFP and FLAG-Sept14CC vectors) in distinct parts of the cerebral cortex (layer II-IV, layer V-VI, IZ, and SVZ/VZ) for each experimental condition. Error bars indicate SD. \* $p < 0.01$ , percentage of cells in each region relative to the corresponding values with control condition.

mechanisms still remain to be elucidated. It is well accepted that directed cell migration and morphological changes are tightly associated with each other and executed by a coordi-

nated regulation of microtubules and actin filaments (Etienne-Manneville, 2004). Indeed, several molecules concerned in microtubule dynamics, such as Doublecortin, LIS1, microtubule-associated protein 1B, c-Jun NH<sub>2</sub>-terminal kinase (JNK), and focal adhesion kinase, have been reported to play important roles in neuronal migration (des Portes *et al.*, 1998; Hirotsune *et al.*, 1998; Takei *et al.*, 2000; Kawauchi *et al.*, 2003; Xie *et al.*, 2003). Regulators of actin cytoskeleton, such as Filamin A, Myosin II, and Cofilin, are also suggested to be involved in neuronal migration (Fox *et al.*, 1998; Schaar and McConnell, 2005; Kawauchi *et al.*, 2006). Given that mammalian septins interact, if not directly, with F-actin as well as microtubules and probably modulate their dynamics in vivo (Adams *et al.*, 1998; Surka *et al.*, 2002; Nagata *et al.*, 2003; Kremer *et al.*, 2005), it is possible that Sept14 and Sept4 are involved in neuronal migration by modulating functions of cytoskeleton-regulating proteins and/or cytoskeleton itself.

It should be noted that the cytoskeleton-related molecules as mentioned above also play important roles in the regulation of neuronal cell morphology (Arimura and Kaibuchi, 2007). In this study, we show that knockdown of Sept14 or Sept4 resulted in shortening of the leading process of migrating cortical neurons (Figure 8, A-D) and defective extension of axon and dendrite in cultured hippocampal neurons (Figure 9, A-C). It is reported that newborn cortical neurons transfected with a dominant-negative version of Rac1 does not form leading processes and that neurons transfected with a dominant-negative version of JNK exhibit short and twisted leading processes (Kawauchi *et al.*, 2003). Because migration defect was consequently observed in both cases, neuronal migration is likely to be related to cell morphology and abnormal cell shape may at least partly contribute to migration defect. Although the molecular basis linking the leading process formation to neuronal migration

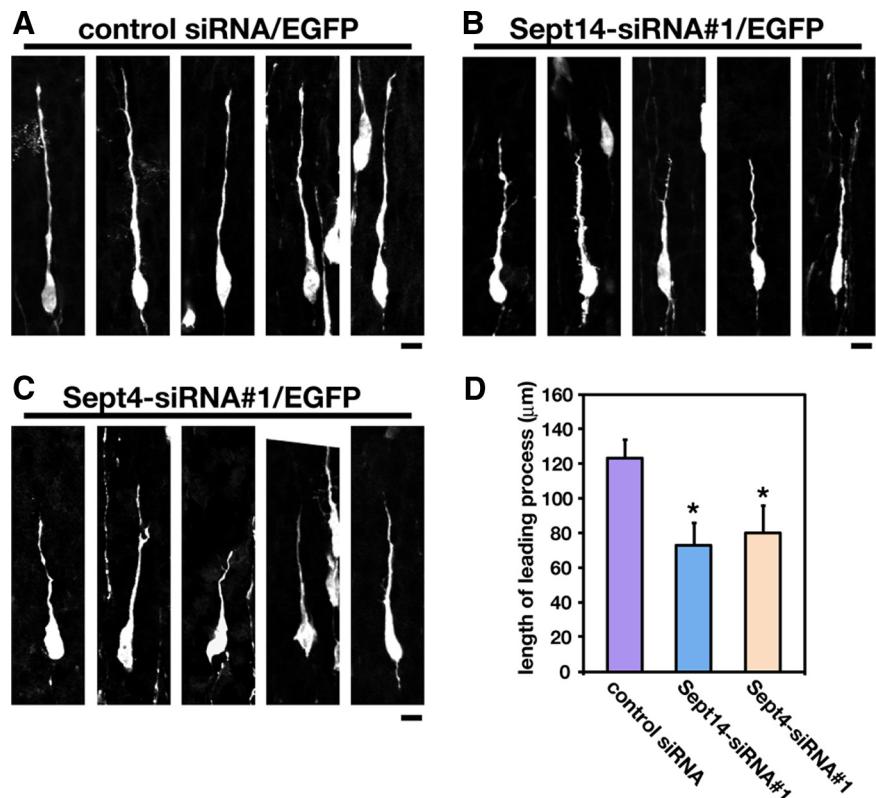


**Figure 8.** Roles of Sept14 and Sept4 in the leading process formation. (A-C) pCAG-EGFP was electroporated with control siRNA (A), Sept14-siRNA#1 (B), or Sept4-siRNA#1 (C) into cerebral cortices at E14.5, followed by fixation at E17.5. Coronal sections were prepared and immunostained with anti-GFP. Five representative images of migrating neurons in the lower CP in each experimental condition were shown. Bars, 20  $\mu$ m. (D) Quantification of the length of the leading process. Numbers of cells used for each calculation are  $>50$ . Error bars indicate SD. \* $p < 0.01$ .

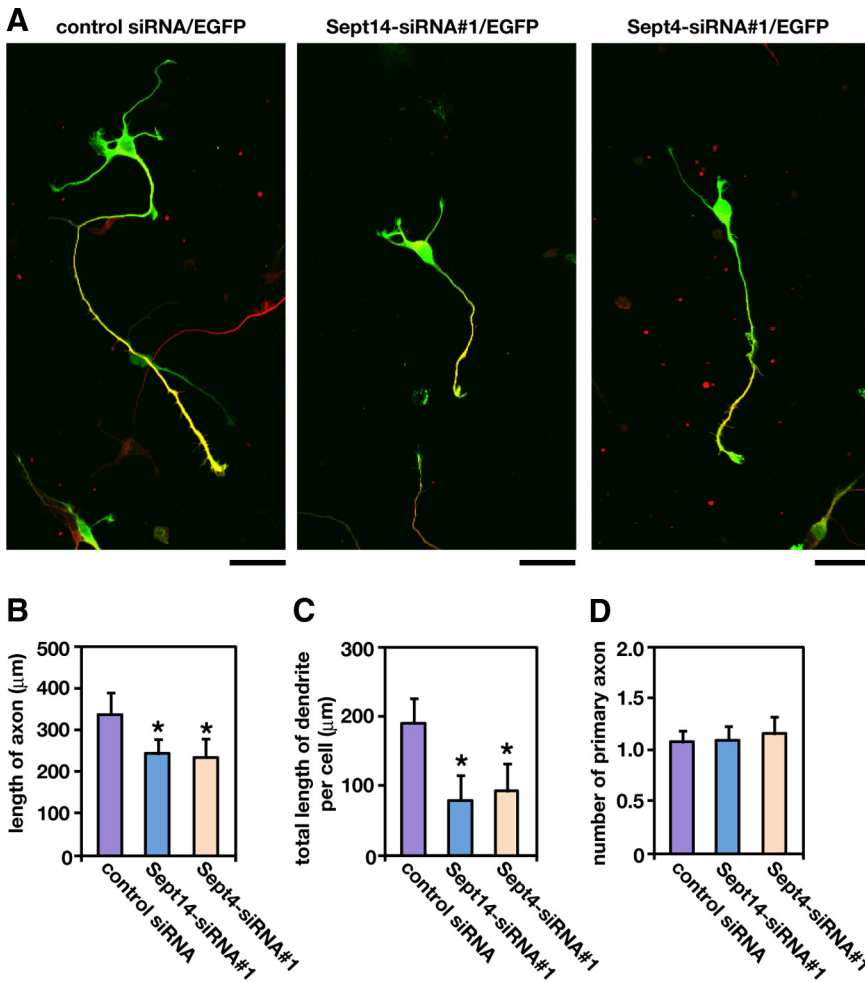


**Figure 9.** Involvement of Sept14 and Sept4 in the process formation in primary cultured hippocampal neurons. (A) Dissociated neurons were obtained from E17.5 mouse, followed by cotransfection of pCAG-EGFP with control siRNA, Sept14-siRNA#1, or Sept4-siRNA#1. After 72 h, cells were fixed and immunostained with anti-GFP (green) and anti-tau-1 (red). Bars, 50  $\mu\text{m}$ . (B–D) Quantifications of the length of primary axon (B), total length of primary dendrites (C), and the number of primary axon per cell (D). Numbers of cells used for each calculation are >50. Error bars indicate SD. \* $p < 0.01$ .

still remains to be elucidated, findings obtained in the present study may support the hypothesis that proper formation of leading process is crucial to coordinated neuronal migration.

Recently, structure models of Sept2 dimer and Sept2/6/7 complex have proposed (Sirajuddin *et al.*, 2007). Based on their x-ray crystallography and electron microscopic observation, these septins have two alternative interacting interfaces, named G-dimer or NC-dimer, and C-terminal coiled-coil regions of Sept2, Sept6, and Sept7 are not likely to be required for their oligomeric complex formation. Conversely, we here propose the importance of the C-terminal coiled-coil region of Sept14 for the interaction with Sept4, at least in our experimental conditions. Because observations obtained in this study could not be simply explained by the G- or NC-dimer model, another mode of interaction, such as coiled-coil-mediated association, might exist in septin oligomerization. It is also possible that Sept14 and Sept4 form a G- or NC-dimer-like complex, although the affinity of coiled-coil-mediated interaction may be much higher in certain physiological conditions. Crystallography and electron microscopic analyses will shed light on the mode of Sept14–Sept4 interaction.

It is notable that Sept4-deficient mice did not show any morphological alteration in cerebral cortex (Ihara *et al.*, 2005; Ihara *et al.*, 2007). Alternatively, we here observed that acute knockdown of Sept4 as well as Sept14 is involved in cortical neuronal migration (Figure 5, C and D). In this

context, conditional and acute knockdown by the combination of in utero electroporation and RNAi is suggested to circumvent the compensatory effects of general gene-knockout approaches. Indeed, Doublecortin- or P27<sup>KIP1</sup>-deficient mice exhibited no obvious morphological alteration in cerebral cortex (Fero *et al.*, 1996; Kiyokawa *et al.*, 1996; Nakayama *et al.*, 1996; Corbo *et al.*, 2002), whereas acute knockdown of these genes by in utero electroporation resulted in defective neuronal migration (Bai *et al.*, 2003; Kawauchi *et al.*, 2006). Considering that many septin molecules including Sept14 are expressed in developing cerebral cortex (Figure 1, B–D; Ito *et al.*, 2009), it is possible that these septins may partially compensate for the function of Sept4 in migrating neurons of Sept4-deficient mice.

It was recently reported that the expression of several septins is up-regulated in the prefrontal cortex of schizophrenic and bipolar patients (Pennington *et al.*, 2008). Intriguingly, Sept5-deficient mice also showed a schizophrenia-related phenotype (Suzuki *et al.*, 2009). It is now widely accepted that the pathogenesis of schizophrenia is related to cortical development, especially of the prefrontal area (Weinberger, 1987). Thus, it is tempting to speculate that defective cortical development induced by the dysfunction of Sept14, Sept4, or other septins may contribute to the onset and/or progress of schizophrenia, although intensive studies are needed to clarify the molecular mechanisms linking pathophysiology of the disease and septins.

## ACKNOWLEDGMENTS

We thank Drs. M. Kinoshita and M. Takehashi for providing cDNAs and antibodies, Drs. M. Hoshino and T. Kawauchi for providing plasmids, and Drs. K. Okamoto and D. Tsuboi for helpful discussions. This work was supported in part by grant-in-aid for young scientists (start-up), scientific research on priority area and scientific research (B) from the Ministry of Education, Culture, Sports, Science and Technology, Japan.

## REFERENCES

- Adams, R. R., Tavares, A. A., Salzberg, A., Bellen, H. J., and Glover, D. M. (1998). Pavarotti encodes a kinesin-like protein required to organize the central spindle and contractile ring for cytokinesis. *Genes Dev.* *12*, 1483–1494.
- Arimura, N., and Kaibuchi, K. (2007). Neuronal polarity: from extracellular signals to intracellular mechanisms. *Nat. Rev. Neurosci.* *8*, 194–205.
- Bai, J., Ramos, R. L., Ackman, J. B., Thomas, A. M., Lee, R. V., and LoTurco, J. J. (2003). RNAi reveals doublecortin is required for radial migration in rat neocortex. *Nat. Neurosci.* *6*, 1277–1283.
- Barral, Y., and Kinoshita, M. (2008). Structural insights shed light onto septin assemblies and function. *Curr. Opin. Cell Biol.* *20*, 12–18.
- Clark, G. D. (2002). Brain development and the genetics of brain development. *Neurol. Clin.* *20*, 917–939.
- Collins, M. O., Husi, H., Yu, L., Brandon, J. M., Anderson, C. N., Blackstock, W. P., Choudhary, J. S., and Grant, S. G. (2006). Molecular characterization and comparison of the components and multiprotein complexes in the postsynaptic proteome. *J. Neurochem.* *97* (suppl 1), 16–23.
- Corbo, J. C., Deuel, T. A., Long, J. M., LaPorte, P., Tsai, E., Wynshaw-Boris, A., and Walsh, C. A. (2002). Doublecortin is required in mice for lamination of the hippocampus but not the neocortex. *J. Neurosci.* *22*, 7548–7557.
- Craig, A. M., and Banker, G. (1994). Neuronal polarity. *Annu. Rev. Neurosci.* *17*, 267–310.
- des Portes, V., et al. (1998). Doublecortin is the major gene causing X-linked subcortical laminar heterotopia (SCLH). *Hum. Mol. Genet.* *7*, 1063–1070.
- Dobbelaere, J., and Barral, Y. (2004). Spatial coordination of cytokinetic events by compartmentalization of the cell cortex. *Science* *305*, 393–396.
- Etienne-Manneville, S. (2004). Actin and microtubules in cell motility: which one is in control? *Traffic* *5*, 470–477.
- Fero, M. L., et al. (1996). A syndrome of multiorgan hyperplasia with features of gigantism, tumorigenesis, and female sterility in p27 (Kip1)-deficient mice. *Cell* *85*, 733–744.
- Field, C. M., and Kellogg, D. (1999). Septins: cytoskeletal polymers or signaling GTPases? *Trends Cell Biol.* *9*, 387–394.
- Finger, F. P., Kopish, K. R., and White, J. G. (2003). A role for septins in cellular and axonal migration in *C. elegans*. *Dev. Biol.* *261*, 220–234.
- Fox, J. W., et al. (1998). Mutations in filamin 1 prevent migration of cerebral cortical neurons in human periventricular heterotopia. *Neuron* *21*, 1315–1325.
- Gleeson, J. G., and Walsh, C. A. (2000). Neuronal migration disorders: from genetic diseases to developmental mechanisms. *Trend Neurosci.* *23*, 352–359.
- Gupta, A., Tsai, L. H., and Wynshaw-Boris, A. (2002). Life is a journey: a genetic look at neocortical development. *Nat. Rev. Genet.* *3*, 342–355.
- Hanai, N., Nagata, K., Kawajiri, A., Shiromizu, T., Saito, N., Hasegawa, Y., Murakami, S., and Inagaki, M. (2004). Biochemical and cell biological characterization of a mammalian septin, Sept11. *FEBS Lett.* *568*, 83–88.
- Hartwell, L. H. (1971). Genetic control of the cell division cycle in yeast. IV. Genes controlling bud emergence and cytokinesis. *Exp. Cell Res.* *69*, 265–276.
- Hatten, M. E. (2002). New directions in neuronal migration. *Science* *297*, 1660–1663.
- Hirotsune, S., Fleck, M. W., Gambello, M. J., Bix, G. J., Chen, A., Clark, G. D., Ledbetter, D. H., McBain, C. J., and Wynshaw-Boris, A. (1998). Graded reduction of Pafah1b1 (Lis1) activity results in neuronal migration defects and early embryonic lethality. *Nat. Genet.* *19*, 333–339.
- Hu, Q., Nelson, W. J., and Spiliotis, E. T. (2008). Forchlorfenuron alters mammalian septin assembly, organization, and dynamics. *J. Biol. Chem.* *283*, 29563–29571.
- Ihara, M., et al. (2005). Cortical organization by the septin cytoskeleton is essential for structural and mechanical integrity of mammalian spermatozoa. *Dev. Cell* *8*, 343–352.
- Ihara, M., et al. (2007). Sept4, a component of presynaptic scaffold and Lewy bodies, is required for the suppression of alpha-synuclein neurotoxicity. *Neuron* *53*, 519–533.
- Inoue, T., and Krumlauf, R. (2001). An impulse to the brain—using in vivo electroporation. *Nat. Neurosci.* *4* (suppl), 1156–1158.
- Ito, H., Kamei, K., Iwamoto, I., Inaguma, Y., García-Mata, R., Sztul, E., and Kato, K. (2002). Inhibition of proteasomes induces accumulation, phosphorylation, and recruitment of HSP27 and alphaB-crystallin to aggregates. *J. Biochem.* *131*, 593–603.
- Ito, H., et al. (2009). Sept8 controls the binding of vesicle-associated membrane protein 2 to synaptophysin. *J. Neurochem.* *108*, 867–880.
- Kawauchi, T., Chihama, K., Nabeshima, Y., and Hoshino, M. (2003). The in vivo roles of STEF/Tiam1, Rac1 and JNK in cortical neuronal migration. *EMBO J.* *22*, 4190–4201.
- Kawauchi, T., Chihama, K., Nishimura, Y. V., Nabeshima, Y., and Hoshino, M. (2005). MAP1B phosphorylation is differentially regulated by Cdk5/p35, Cdk5/p25, and JNK. *Biochem. Biophys. Res. Commun.* *331*, 50–55.
- Kawauchi, T., Chihama, K., Nabeshima, Y., and Hoshino, M. (2006). Cdk5 phosphorylates and stabilizes p27kip1 contributing to actin organization and cortical neuronal migration. *Nat. Cell Biol.* *8*, 17–26.
- Kinoshita, A., Kinoshita, M., Akiyama, H., Tomimoto, H., Akiguchi, I., Kumar, S., Noda, M., and Kimura, J. (1998). Identification of septins in neurofibrillary tangles in Alzheimer's disease. *Am. J. Pathol.* *153*, 1551–1560.
- Kinoshita, A., Noda, M., and Kinoshita, M. (2000). Differential localization of septins in the mouse brain. *J. Comp. Neurol.* *428*, 223–239.
- Kinoshita, M., Kumar, S., Mizoguchi, A., Ide, C., Kinoshita, A., Haraguchi, T., Hiraoka, Y., and Noda, M. (1997). Nedd5, a mammalian septin, is a novel cytoskeletal component interacting with actin-based structures. *Genes Dev.* *11*, 1535–1547.
- Kiyokawa, H., Kineman, R. D., Manova-Todorova, K. O., Soares, V. C., Hoffman, E. S., Ono, M., Khanam, D., Hayday, A. C., Frohman, L. A., and Koff, A. (1996). Enhanced growth of mice lacking the cyclin-dependent kinase inhibitor function of p27 (Kip1). *Cell* *85*, 721–732.
- Kremer, B. E., Haystead, T., and Macara, I. G. (2005). Mammalian septins regulate microtubule stability through interaction with the microtubule-binding protein MAP4. *Mol. Biol. Cell* *16*, 4648–4659.
- Li, X., Serwanski, D. R., Miralles, C. P., Nagata, K., and De Blas, A. (2009). Septin 11 is present in GABAergic synapses and plays a functional role in the cytoarchitecture of neurons and GABAergic synaptic connectivity. *J. Biol. Chem.* *284*, 17253–17265.
- Lew, D. J. (2003). The morphogenesis checkpoint: how yeast cells watch their figures. *Curr. Opin. Cell Biol.* *15*, 648–653.
- Longtine, M. S., DeMarini, D. J., Valencik, M. L., Al-Awar, O. S., Fares, H., De Virgilio, C., and Pringle, J. R. (1996). The septins: roles in cytokinesis and other processes. *Curr. Opin. Cell Biol.* *8*, 106–119.
- Low, C., and Macara, I. G. (2006). Structural analysis of septin 2, 6, and 7 complexes. *J. Biol. Chem.* *281*, 30697–30706.
- Nagata, K., Puls, A., Futter, C., Aspenstrom, P., Schaefer, E., Nakata, T., Hirokawa, N., and Hall, A. (1998). The MAP kinase kinase MLK2 co-localizes with activated JNK along microtubules and associates with kinesin superfamily motor KIF3. *EMBO J.* *17*, 149–158.
- Nagata, K., Kawajiri, A., Matsui, S., Takagishi, M., Shiromizu, T., Saitoh, N., Izawa, I., Kiyono, T., Itoh, T. J., Hotani, H., and Inagaki, M. (2003). Filament formation of MSF-A, a mammalian septin, in human mammary epithelial cells depends on interactions with microtubules. *J. Biol. Chem.* *278*, 18538–18543.
- Nagata, K., Asano, T., Nozawa, Y., and Inagaki, M. (2004). Biochemical and cell biological analyses of a mammalian septin complex, Sept7/9b/11. *J. Biol. Chem.* *279*, 55895–55904.
- Nakayama, K., Ishida, N., Shirane, M., Inomata, A., Inoue, T., Shishido, N., Horii, I., Loh, D. Y., and Nakayama, K. (1996). Mice lacking p27 (Kip1) display increased body size, multiple organ hyperplasia, retinal dysplasia, and pituitary tumors. *Cell* *85*, 707–720.
- Nguyen, T. Q., Sawa, H., Okano, H., and White, J. G. (2000). The *C. elegans* septin genes, *unc-59* and *unc-61*, are required for normal postembryonic cytokinesis and morphogenesis but have no essential function in embryogenesis. *J. Cell Sci.* *113*, 3825–3837.
- Noctor, S. C., Martínez-Cerdeño, V., Ivic, L., and Kriegstein, A. R. (2004). Cortical neurons arise in symmetric and asymmetric division zones and migrate through specific phases. *Nat. Neurosci.* *7*, 136–144.
- Oegema, K., Desai, A., Wong, M. L., Mitchison, T. J., and Field, C. M. (1998). Purification and assay of a septin complex from *Drosophila* embryos. *Methods Enzymol.* *298*, 279–295.
- Olson, E. C., and Walsh, C. A. (2002). Smooth, rough and upside-down neocortical development. *Curr. Opin. Genet. Dev.* *12*, 320–327.

- Peng, J., Kim, M. J., Cheng, D., Duong, D. M., Gygi, S. P., and Sheng, M. (2004). Semiquantitative proteomic analysis of rat forebrain postsynaptic density fractions by mass spectrometry. *J. Biol. Chem.* *279*, 21003–21011.
- Pennington, K., Beasley, C. L., Dicker, P., Fagan, A., English, J., Pariante, C. M., Wait, R., Dunn, M. J., and Cotter, D. R. (2008). Prominent synaptic and metabolic abnormalities revealed by proteomic analysis of the dorsolateral prefrontal cortex in schizophrenia and bipolar disorder. *Mol. Psychiatry* *13*, 1102–1117.
- Peterson, E. A., Kalikin, L. M., Steels, J. D., Estey, M. P., Trimble, W. S., and Petty, E. M. (2007). Characterization of a SEPT9 interacting protein, SEPT14, a novel testis-specific septin. *Mamm. Genome* *18*, 796–807.
- Rakic, P. (1990). Principles of neural cell migration. *Experientia* *46*, 882–891.
- Saito, T., and Nakatsuji, N. (2001). Efficient gene transfer into the embryonic mouse brain using *in vivo* electroporation. *Dev. Biol.* *240*, 237–246.
- Schaar, B. T., and McConnell, S. K. (2005). Cytoskeletal coordination during neuronal migration. *Proc. Natl. Acad. Sci. USA* *102*, 13652–13657.
- Scheffield, P. J., Oliver, C. J., Kremer, B. E., Sheng, S., Shao, Z., and Macara, I. G. (2003). Borg/septin interactions and the assembly of mammalian septin heterodimers, trimers, and filaments. *J. Biol. Chem.* *278*, 3483–3488.
- Shinoda, T., Taya, S., Tsuboi, D., Hikita, T., Matsuzawa, R., Kuroda, S., Iwamatsu, A., and Kaibuchi, K. (2007). DISC1 regulates neurotrophin-induced axon elongation via interaction with Grb2. *J. Neurosci.* *27*, 4–14.
- Sirajuddin, M., Farkasovsky, M., Hauer, F., Kühlmann, D., Macara, I. G., Weyand, M., Stark, H., and Wittinghofer, A. (2007). Structural insight into filament formation by mammalian septins. *Nature* *449*, 311–315.
- Spiliotis, E. T., and Nelson, W. J. (2006). Here come the septins: novel polymers that coordinate intracellular functions and organization. *J. Cell Sci.* *119*, 4–10.
- Surka, M. C., Tsang, C. W., and Trimble, W. S. (2002). The mammalian septin MSF localizes with microtubules and is required for completion of cytokinesis. *Mol. Biol. Cell* *13*, 3532–3545.
- Suzuki, G., *et al.* (2009). Sept5 deficiency exerts pleiotropic influence on affective behaviors and cognitive functions in mice. *Hum. Mol. Genet.* *18*, 1652–1660.
- Tabata, H., and Nakajima, K. (2001). Efficient *in utero* gene transfer system to the developing mouse brain using electroporation: visualization of neuronal migration in the developing cortex. *Neuroscience* *103*, 865–872.
- Tabata, H., and Nakajima, K. (2003). Multipolar migration: the third mode of radial neuronal migration in the developing cerebral cortex. *J. Neurosci.* *23*, 9996–10001.
- Tada, T., Simonetta, A., Batterton, M., Kinoshita, M., Edbauer, D., and Sheng, M. (2007). Role of Septin cytoskeleton in spine morphogenesis and dendrite development in neurons. *Curr. Biol.* *17*, 1752–1758.
- Takei, Y., Teng, J., Harada, A., and Hirokawa, N. (2000). Defects in axonal elongation and neuronal migration in mice with disrupted tau and map1b genes. *J. Cell Biol.* *150*, 989–1000.
- Takizawa, P. A., DeRisi, J. L., Wilhelm, J. E., and Vale, R. D. (2000). Plasma membrane compartmentalization in yeast by messenger RNA transport and a septin diffusion barrier. *Science* *290*, 341–344.
- Trimble, W. S. (1999). Septins: a highly conserved family of membrane-associated GTPases with functions in cell division and beyond. *J. Membr. Biol.* *169*, 75–81.
- Weinberger, D. R. (1987). Implications of normal brain development for the pathogenesis of schizophrenia. *Arch. Gen. Psychiatry* *44*, 660–669.
- Xie, Y., Vessey, J. P., Konecna, A., Dahm, R., Macchi, P., and Kiebler, M. A. (2007). The GTP-binding protein Septin 7 is critical for dendrite branching and dendritic-spine morphology. *Curr. Biol.* *17*, 1746–1751.
- Xie, Z., Sanada, K., Samuels, B. A., Shih, H., and Tsai, L. H. (2003). Serine 732 phosphorylation of FAK by Cdk5 is important for microtubule organization, nuclear movement, and neuronal migration. *Cell* *114*, 469–482.
- Xue, J., Tsang, C. W., Gai, W. P., Malladi, C. S., Trimble, W. S., Rostas, J. A., and Robinson, P. J. (2004). Septin 3 (G-septin) is a developmentally regulated phosphoprotein enriched in presynaptic nerve terminals. *J. Neurochem.* *91*, 579–590.